PAPER

Mononuclear gold(III) complexes with diazanaphthalenes: the influence of the position of nitrogen atoms in the aromatic rings on the complex crystalline properties†

Biljana Đ. Glišić, [ID] *[a] Beata Warżajtis, [ID] [b] Marcin Hoffmann, [ID] [b] Urszula Rychlewska [ID] [b] and Miloš I. Djuran [ID] [c]

A series of mononuclear gold(III) complexes of the general formula [AuCl₃(diazanaphthalene)], where diazanaphthalene is quinazoline (qz, **1**), phthalazine (phtz, **2**), 1,5-naphthyridine (1,5-naph, **3**), 1,6-naphthyridine (1,6-naph, **4**) or 1,8-naphthyridine (1,8-naph, **5**), were prepared and fully characterized. The complexes **1–5** consist of discrete monomeric species with the Au(III) cation in a square planar coordination geometry surrounded by three chloride anions and one diazanaphthalene ligand. Crystallographic studies indicate the presence of an extended 4 + 1 or 4 + 2 geometry around the square planar [AuCl₃(diazanaphthalene)] center due to Au⋯Cl and Au⋯N interactions. The crystal structures of these complexes are controlled by a variety of intermolecular interactions that utilize the amphiphilic properties of the coordinated chloride anions and involve C–H groups, π-electrons, and an uncoordinated nitrogen atom of the diazanaphthalene ligand. The usual offset π-stacking between the N-heteroaromatic ligands appears to be completely hindered between the 1,5-naph fragments and significantly weakened between the 1,6-naph and 1,8-naph in their respective complexes **3**, **4** and **5**, for which the average molecular polarizability (α) values are the lowest in the series. It is remarkable that the [AuCl₃(benzodiazine)] complexes **1** and **2** form centrosymmetric crystals, but the [AuCl₃(naphthyridine)] complexes **3–5** assemble into non-centrosymmetric aggregates, making them potential alternatives to the previously studied systems for application in various fields by taking advantage of their polarity.

Introduction

The observed interest in the coordination chemistry of gold(III) with aromatic nitrogen-containing heterocyclic ligands (N-heterocycles) has several reasons. N-Heterocycles are of great biological significance, since they can be found in many bioactive natural products, as well as medicinally and biologically important compounds.[1,2] For example, one can mention a porphyrin ring in haemoglobin, which consists of four pyrrole molecules cyclically linked together, a corrin ring in vitamin B₁₂, and purine and pyrimidine bases which are found in DNA and RNA structures. Besides that, N-heterocycles containing donor–acceptor substitution have been shown to exhibit unique photophysical and photochemical properties owing to the

charge transfer. For example, 1,6-naphthyridine derivatives were reported as a new class of compounds for nonlinear optics.[3] Due to their structural properties, N-heterocycles provide rigid building blocks for molecular architectures with various transition metals,[4–6] so they have been extensively utilized for the formation of numerous mononuclear and polynuclear metal complexes,[7–12] metallosupramolecular assemblies with desirable structures and properties,[13] as well as for the construction of structural and functional models of metalloenzyme active sites.[14–16]

Another important reason for investigation of gold(III) chemistry with N-heterocycles stems from the finding that use of these ligands in the synthesis of gold(III) complexes enhances the stability of Au(III) ion under physiological conditions, allowing evaluation of gold(III) complexes as potential antitumor[17] and antimicrobial agents.[18] Thus, different N-heterocycles such as pyridine, bipyridine, terpyridine, phenanthroline and porphyrins have been used and a number of mononuclear and dinuclear gold(III) complexes have been synthesized showing cytotoxic activity toward different human tumor cell lines,[19–28] as well as significant activity against the microbes[29] and the parasites which are causative agents of
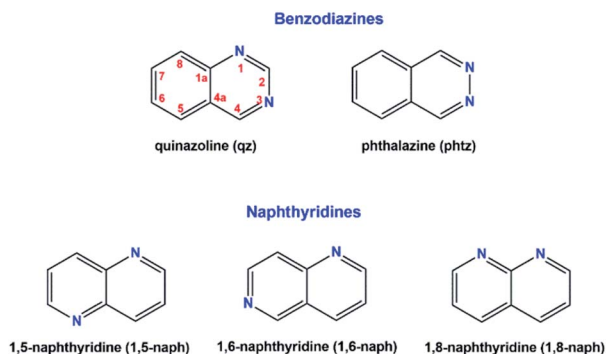
ᵃUniversity of Kragujevac, Faculty of Science, Department of Chemistry, R. Domanovića 12, 34000 Kragujevac, Serbia. E-mail: biljana.glisic@pmf.kg.ac.rs

ᵇFaculty of Chemistry, Adam Mickiewicz University in Poznań, Uniwersytetu Poznańskiego 8, 61-614 Poznań, Poland

ᶜSerbian Academy of Sciences and Arts, Knez Mihailova 35, 11000 Belgrade, Serbia

Scheme 1 Schematic drawing of diazanaphthalene ligands used in the present study. The numbering of atoms used for NMR assignation follows the IUPAC rules and does not match the one applied in the X-ray and theoretical studies of gold(III) complexes with these ligands. The α positions are numbered 1, 4, 5 and 8, while the β positions are 2, 3, 6 and 7.

tropical diseases, such as malaria,[30] leishmaniasis[31,32] and trypanosomiasis.[33,34]

In the light of the abovementioned, we have already reported the synthesis, NMR and X-ray structural characterization of mononuclear gold(III) complexes with some diazaaromatics, namely pyridazine, pyrimidine, pyrazine, quinoxaline, phenazine, 1,7-phenanthroline and 4,7-phenanthroline, [AuCl₃(N-heterocycle)].[35–37] All complexes were obtained by reacting K[AuCl₄] and the corresponding N-heterocycle in 1 : 1 molar ratio in the mixture of water and ethanol or in the pure ethanol. Furthermore, we have synthesized a new class of N-heterocycles based on camphorquinoxaline core and the corresponding mononuclear gold(III) complexes.[38] By fusing the quinoxaline with camphor moiety, we have made the two nitrogen binding sites nonequivalent in order to investigate which of the two nitrogen atoms will be involved in the formation of mononuclear complexes, and found out that the investigated camphoquinoxaline derivatives had encoded information, both spatial and directional, that led to the formation of single coordination products, in which Au(III) ion is bound to the less sterically hindered of the two nonequivalent nitrogen atoms.[38]

In the course of the above investigations[35–38] and in order to test the possible changes in the approach of nitrogen heterocycles with extended annelated π systems, we report herein the synthesis, spectroscopic and X-ray crystallographic characterization of gold(III) complexes with five diazanaphthalene ligands (Scheme 1). Density functional theory (DFT) calculations were performed in order to gain more insight into the coordination mode of diazanaphthalenes toward Au(III) ion.

Results and discussion

In the present study, we have investigated the coordination ability of five diazanaphthalenes, namely quinazoline (qz), phthalazine (phtz), 1,5-naphthyridine (1,5-naph), 1,6-naphthyridine (1,6-naph) and 1,8-naphthyridine (1,8-naph) (Scheme 1) toward Au(III) ion. Two of the five presently investigated diazanaphthalene ligands, qz and phtz, contain nitrogen atoms

within the same ring, hence they belong to a group of benzodiazines, while the remaining three, *i.e.* 1,5-naph, 1,6-naph and 1,8-naph, contain nitrogen atoms in different rings and are classified to naphthyridines. As in naphthalene, in the diazanaphthalene isomers, one can distinguish two nonequivalent sites α and β at which a nitrogen atom can be placed, and to either of which the Au–N bond may be formed. As a consequence, in the diazanaphthalene ligands one can have the two nitrogen atoms either placed at different sites α and β (qz and 1,6-naph), or at the same site, β (phtz) or α (1,5-naph and 1,8-naph). It appears that, despite of the different steric and electronic properties of the investigated diazanaphthalenes, their reactions with [AuCl₄]⁻ invariably lead to the formation of mononuclear [AuCl₃(qz)] (**1**), [AuCl₃(phtz)] (**2**), [AuCl₃(1,5-naph)] (**3**), [AuCl₃(1,6-naph)] (**4**) and [AuCl₃(1,8-naph)] (**5**) complexes having one monodentatedly coordinated diazanaphthalene ligand, regardless the different ratio of the used substrates. In this respect, they behave similarly to the previously investigated quinoxaline, another isomer of diazanaphthalene,[36] and to camphorquinoxaline derivatives.[38] In two of the five ligands, namely qz and 1,6-naph, the potential metal binding nitrogen atoms are nonequivalent (α and β), therefore it is legitimate to pose a question which of the two nitrogen atoms will be subjected to the attack of the Au(III) electrophile.

Structural characterization of gold(III) complexes 1–5

Crystal structure description. Details of the data collection parameters and refinement of the structures of **1–5** are presented in Table S1.† Key bond lengths and bond angles for these complexes have been included in Table S2.† The structure of the investigated molecules as found in the solid state is displayed in Fig. 1.

The crystal structure of all these complexes consists of discrete monomeric species with the Au(III) in a square planar coordination geometry surrounded by three chloride anions and only one diazanaphthalene ligand. In this respect, **3** constitutes the first example of the crystal structure, where only one nitrogen atom of the 1,5-naph ligand has been involved in the coordination to the metal ion. As the search of the CSD (Cambridge Structural Database) reveals,[39] in the previously reported metal complexes, in which the 1,5-naph acts as a ligand, it always utilizes both nitrogen atoms to form coordination bonds in a bidentate-bridging mode, which results in the formation of 1D coordination polymers. As a consequence of the coordination of only one of the two diazanaphthalene nitrogen atoms, in each of the investigated complexes the second nitrogen atom of diazanaphthalene remains uncoordinated and is preferably utilized as an acceptor of C–H···N intermolecular hydrogen bond, with the exception of **2**, in which the uncoordinated nitrogen atom N3 makes a close contact of 3.389(4) Å with the neighboring Au(III) ion (symmetry transformation 1 − x, −y, 1 − z). The qz and 1,6-naph ligands possess two alternative and distinguishable nitrogen atoms, to either of which a coordination bond may be formed during the reaction with K[AuCl₄]. It appears that in the respective complexes **1** and **4**, the nitrogen atom at the β site coordinates
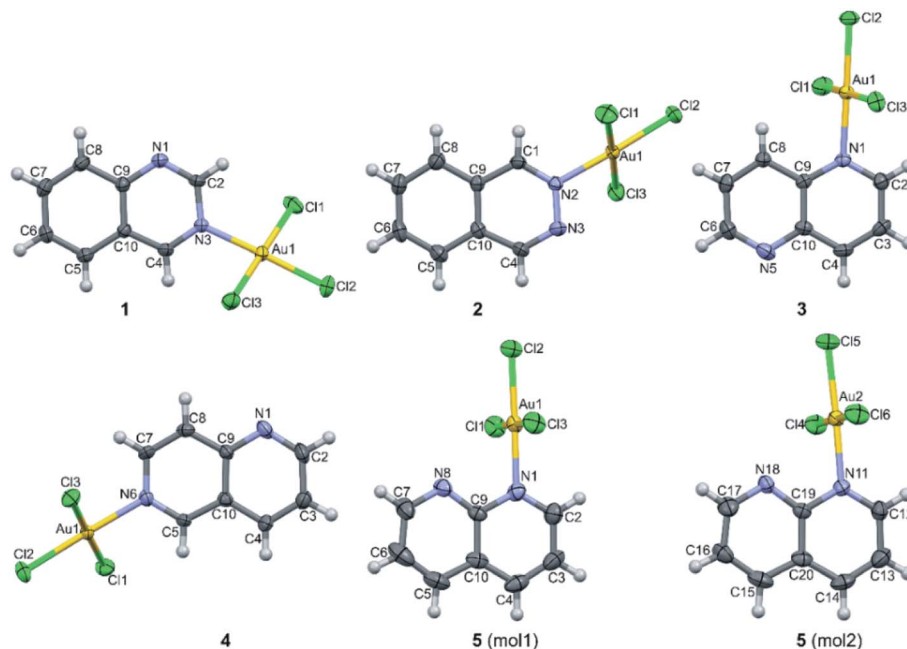
Fig. 1 Molecular structures of five [AuCl$_3$(diazanaphthalene)] complexes showing atomic displacement parameters at 50% probability, except for the hydrogen atoms which were drawn in an arbitrary scale.

to the metal center. This allows the long axis of the ligand to point outward from the coordination plane and get involved in columnar stacking interactions. Fig. 2, which is an overlap of the molecules **3** and **4**, illustrates the relative orientation of the heterocyclic rings with respect to the coordination plane in the complexes, where the ligand is coordinated *via* the α or β nitrogen, respectively.

In all investigated crystal structures, the Au–Cl2 bond which is *trans* with respect to the Au–N bond, is consistently shorter than the remaining Au–Cl1 and Au–Cl3 bonds (for numbering scheme see Fig. 1), which might be considered as an indirect consequence of the higher *trans* effect of the chloride compared to the diazanaphthalene nitrogen atom. The corresponding Au–N bond lengths vary from 2.027(4) to 2.057(8) Å, with the shortest one being in the complex **2**. The values of the valence angles around the coordinated nitrogen atom spread a wide range from 115.8(6) to 124.4(7)° in complexes **2** and **5**, become

more equally distributed in complexes **1** and **3** and almost equal in complex **4** (Table S2†). The mean value of the valence angle at the uncoordinated nitrogen atom equal to 116.8(1.3)° is characteristic for the heterocyclic nitrogen possessing free electron pair.

The complexes **1**–**5** differ in the orientation of the azaaromatic ring plane with respect to the plane defined by the four donor atoms surrounding the Au(III) ion. In the crystals of **5**, the two planes are perpendicular (89.98(10) and 89.30(9)° for two independent molecules), they are somewhat inclined in the crystals of **3** (68.84(7)°), and achieve the values of 62.76(7) and 59.46(9)° in the crystals of **2** and **4**, respectively, while in the crystals of **1**, this interplanar angle is only 39.47(5)°.

Noticeable inclination of the N-heteroaromatic ring with respect to the coordination plane is a source of molecular helicity, which becomes meaningful in the chiral crystals formed by the molecules of **4**. The complexes **1** and **2** that contain benzodiazines as ligands, form triclinic centrosymmetric crystals, in which the dominant intermolecular interactions operate between molecules related by inversion. In contrast, the complexes containing the naphthyridine ligands crystallize either in polar (**3** and **5**) or chiral (**4**) space group. The amphiphilic nature of the charge distribution on the chloride anion coordinated to the Au(III) cation allows it to serve as a Lewis base in Cl···Au interactions (Table S3†), as both a donor and acceptor in Cl···Cl halogen bond (Table S3†) and also as a hydrogen bond acceptor (Table S4†). As a result, in each of the investigated crystals (**1**–**5**), the square planar coordination around Au(III) is extended to square pyramidal or tetragonal bipyramidal due to the Au···Cl intermolecular interactions and the molecular packing is dominated by the intermolecular C–H···Cl hydrogen bonds, which outnumber the other types of the specific
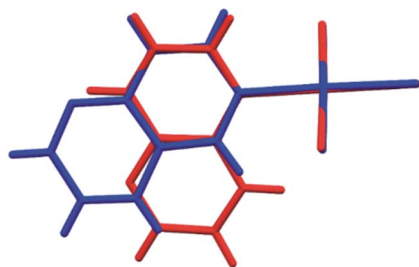

Fig. 2 Overlap of the molecules **3** (red) and **4** (blue) illustrates the relative orientation of the heterocyclic rings with respect to the coordination plane in complexes, where the ligand is coordinated *via* α and β nitrogen, respectively.

intermolecular interactions. Notably, the $\pi\cdots\pi$ stacking interactions play a significant structural role only in the centrosymmetric crystals of $[AuCl_3(benzodiazine)]$ complexes (**1** and **2**) and become either much weaker or completely absent in a series of $[AuCl_3(naphthyridine)]$ crystals (**3–5**). Geometrical parameters describing the $\pi\cdots\pi$ stacking interactions are listed in Table S5.†

In the crystals of **1**, the quinazoline ligand is coordinated to the Au(III) ion via the β nitrogen atom. This allows for the columnar stacking interactions. In the two-ring π-systems, such as benzodiazines, the offset $\pi\cdots\pi$ stacking interaction may involve two nitrogen-containing aromatic rings, two arene rings or the arene and the N-heteroaromatic rings. And indeed, in the crystals of **1**, there are two types of stacking in each column: one involves the pyrimidine and arene moieties of the inversion related quinazoline ligands, while the other encompasses solely the arene rings generated by another set of the inversion centers (Fig. 3a and b). There is a slight preference for the pyrimidine$\cdots$arene approach, followed by the arene$\cdots$arene approach (Table S5†), while pyrimidine$\cdots$pyrimidine type of interactions is nonexistent. Moreover, in the crystals of **1**, one chlorido ligand approaches the Au(III) center at a distance of only 3.295(2) Å, while the sum of the van der Waals radii of the two atoms

amounts to 3.41 Å. The approach of the chloride ion from the other side appears at far longer distance of 3.665(2) Å. Pairs of Au$\cdots$Cl interactions form centrosymmetric dimer (Fig. 3). On both sides of this dimer, there are the quinazoline ligands that are engaged in columnar $\pi\cdots\pi$ stacking interactions. Another supramolecular motif joining molecules related by inversion is the $R_2^2(6)$ ring (graph set notation[40]), formed by a pair of inversion related C2–H2$\cdots$N1 $(2 - x, -y, 1 - z)$ hydrogen bonds involving the uncoordinated nitrogen atom as an acceptor (Table S4†). The appearance of such type of hydrogen bond has been previously noted in gold(III) complexes with pyridazine and pyrimidine monodentatedly coordinated to the metal center[35] and in the crystal structure of gold(III) complex with quinoxaline.[36] Moreover, the Au1–Cl1$\cdots$Cl3 $(x + 1, y, z)$ and Au1–Cl3$\cdots$Cl3 $(-x + 1, -y + 1, -z + 2)$ contacts indicate the presence of type I halogen bonding (see Table S3†).[41]

The packing of **2** is dominated by two features. First, the pairs of complex molecules related by inversion stack off-face at a distance 3.447 Å between the arene and pyridazine moieties (Fig. 4 and Table S5†). Second, the connection between the dimers takes place by means of pairs of inversion-related Au$\cdots$Cl3 and Au$\cdots$N3 interactions at distances of 3.530(2) and 3.389(4) Å, respectively. In this way the coordination sphere
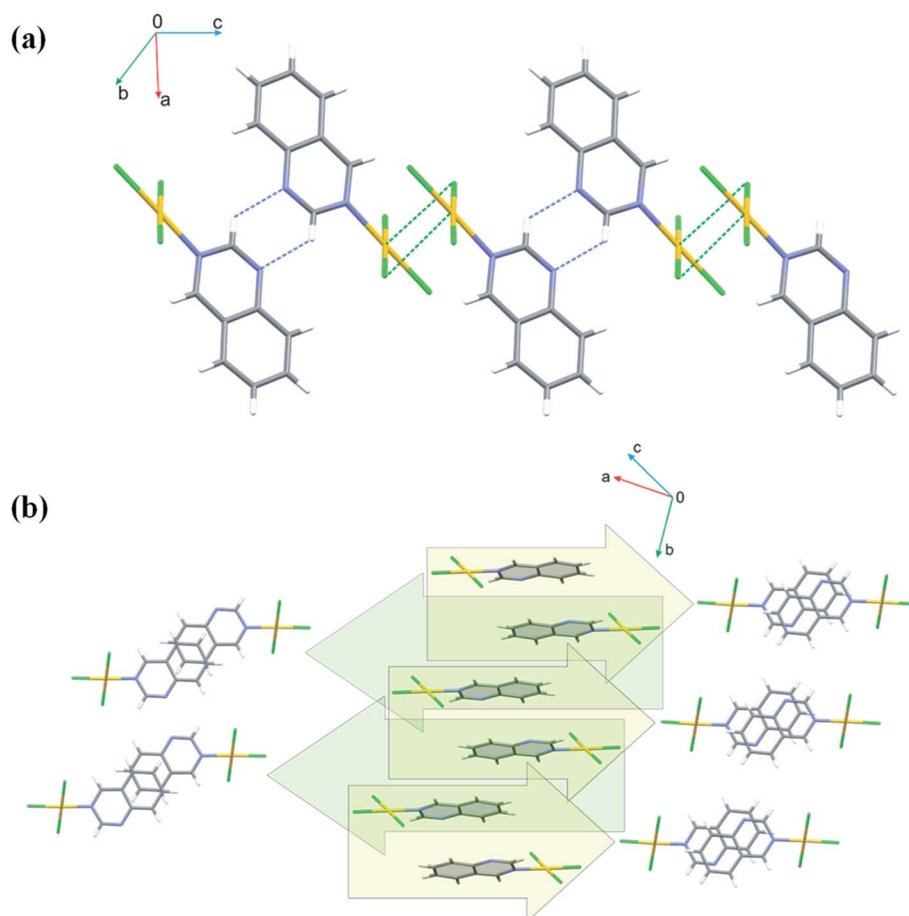

Fig. 3 Packing of the molecules of **1**. The figure illustrates pairs of the centrosymmetric dimers formed via C–H$\cdots$N hydrogen bonds and Au$\cdots$Cl interactions (a); columnar $\pi\cdots\pi$ stacking, and two different modes of molecular overlap within the column (b).
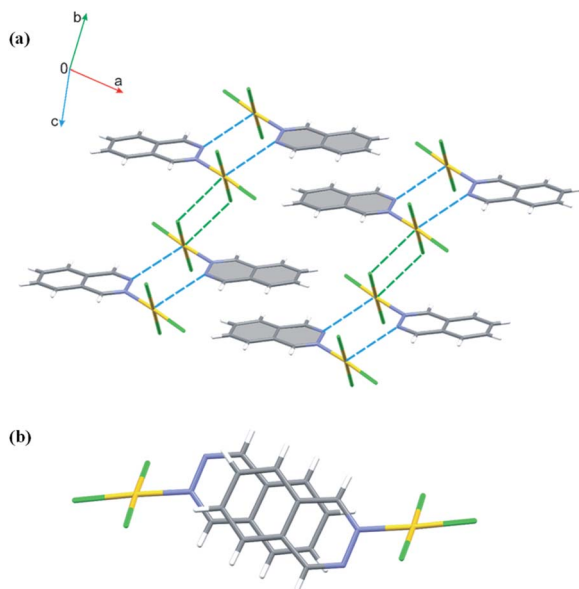
Fig. 4 Packing of the molecules of **2** demonstrating pairs of inversion related Au···N and Au···Cl as well as dimeric π···π stacking interactions (a); view perpendicular to phtz plane displaying a degree of the ring overlap (b).

around Au(III) ion is supplemented to tetragonal bipyramidal (4 + 2). The presence of Au···N3 interactions is unique in the group of [AuCl₃(N-heterocycle)] complexes. Moreover, the Au1–Cl3··· Cl1–Au1 contact of 3.444(2) Å indicates the presence of type I halogen bonding.[41]

As was previously noted,[42] aromatic nitrogen-containing heterocycles are electron poor systems and a metal which is coordinated to a nitrogen heteroatom will further enhance the electron-withdrawing effect through its positive charge. Hence, aromatic nitrogen-containing heterocycles should in principle be well suited for π···π interactions, because of their low π-electron density. In spite of this expectation, the crystals of **3** are deprived of any off-face stacking interactions. The complex molecules interact via C–H···N hydrogen bonds and the Au··· Cl3 interactions, as illustrated in Fig. 5. The azaarene rings, rather than forming the π···π stacking, are engaged in (Cl2)···π interactions. The distance between Cl2 and the center of gravity (C_g) of the C9–C10 bond (symmetry operation $-\frac{1}{2} + x, \frac{1}{2} - y, z$) is 3.386 Å and the Au–Cl···C_g angle amounts to 113.1°. There are also several Cl···Cl interactions operating along the polar z-axis, but geometrical parameters describing these interactions do not allow their straightforward classification into one of the two types of halogen bonds (Table S3†).[43] The complete lack of π···π stacking interactions in crystals containing 1,5-naph as a ligand has been observed by us in 1D polymeric crystals formed by [ZnCl₂(1,5-naph)]ₙ complex, in which the ligand acts in a bidentate-bridging mode and is involved in anion···π interactions.[44]

Crystals of **4** are both polar and chiral. Contrary to the anti-parallel arrangement of the molecules involved in the π···π stacking interactions in the crystals of **1** and **2**, in the crystals of **4** the molecules engaged in stacking are related by single lattice
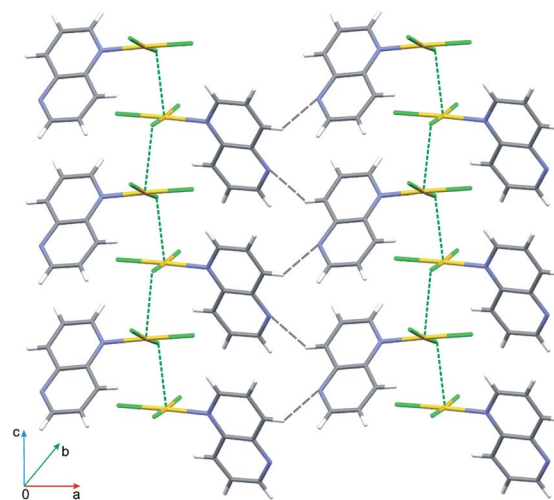

Fig. 5 View of the aggregation in crystals of complex **3** in non-centrosymmetric space group *Pna*2₁. Note the arrangement of molecules along the polar c-direction held together by C−H···N and Au···Cl interactions.

translation along the a-direction, so they stack parallel to each other (Fig. 6). Geometrical parameters describing this type of interactions are less favorable than in the previous two cases (Fig. 6 and Table S5†). The Au(III) ion is approached by two chloride ions at distances 3.427(3) and 3.378(3) Å, extending its coordination sphere to tetragonal bipyramid (4 + 2). Pairwise Au···Cl1 and Au···Cl3 interactions lead to the formation of dimers that mimic those formed around an inversion center in the centrosymmetric crystals of **1** and **2** (Fig. 6).

The molecules of **5** crystallize in the non-centrosymmetric space group *Cc* with two symmetry independent molecules. The coordination of 1,8-naph molecule is monodentate and the
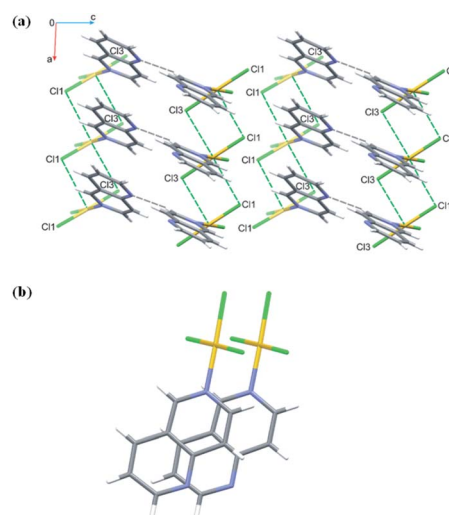

Fig. 6 Arrangement of the molecules of **4** in chiral and polar space group *P*2₁ by means of C−H···N, pairwise Au···Cl1 and Au···Cl3 interactions and columnar stacking along the a-direction (a); view perpendicular to the 1,6-naph plane displaying a small degree of the ring overlap (b).

interaction with the most distant nitrogen atom is minimized, as the angle between the plane of the naph moiety and the coordination plane is close to 90° (*vide supra*). In spite of that, there is probably some interaction between the distant nitrogen and the central Au atom (the Au···N distances are 2.942(6) and 2.901(6) Å in the two symmetry independent molecules) which is of steric importance, because it prevents the approach of another ligand from this side, thus hindering a possibility of extension of the square planar coordination around the Au(III) cation. However, the approach of the chloride anion is still possible from the other side of the coordination plane, which supplements the coordination around Au(III) to square pyramidal (4 + 1).

Two independent molecules of complex **5** display the same geometry and are related by a pseudo-center of symmetry having the approximate fractional *x*, *y*, *z* coordinates of 0.28, 0.39 and 0.35. The two molecules are held together by relatively weak π···π interactions (Table S5†). The dimeric motif is further extended along *b*-direction by means of Au···Cl interactions (Fig. 7) and propagates along *a*-direction by means of C–H···N hydrogen bonds, but overwhelming are the C–H···Cl interactions which operate in all three-dimensions (Table S4†). Using the standard settings inserted to the Mercury program,[45] we were able to identify small voids between the molecular layers parallel to the (001) lattice planes. Multiplication of the number of symmetry independent molecules and the appearance of the structural voids are the signs that the molecule of **5** exhibits difficulties with packing in the crystal. This is also reflected in the values of the crystal density and the Kitajgorodskij packing index,[46] which are the smallest within the investigated series (Table S1†).

Since the work of Kitaigorodskij,[46] it has been recognized that inversion centers in space groups are "good" for the close-packing of molecules. This does not seem to be reflected in the present study. Except for the molecule of **5**, which crystallizes in polar space group *Cc* and exhibits some packing problems in crystal, the remaining crystals display similar values of the calculated density and packing index (Table S1†), despite the fact that some of them form centrosymmetric crystals but some do not. Our observations seem to indicate that the presence of an inversion center is needed for good stacking rather than good packing: the π···π stacking interactions in non-centrosymmetric crystals of **4** and **5** are relatively weak compared with those operating in centrosymmetric crystals of **1** and **2**. Despite the fact that the centrosymmetric space groups are more favored than non-centrosymmetric, the naphthyridine ligands, for some reason, are well suited for the formation of the non-centrosymmetric aggregates. This observation might perhaps be of interest to the non-linear optics community, where the non-centrosymmetric space groups are a requirement.

Spectroscopic characterization. Ambient temperature NMR spectra of gold(III) complexes **1–5**, alongside the diazanaphthalene ligands, were measured in acetone-d_6. The corresponding ^{1}H and ^{13}C chemical shifts are listed in the Experimental section. It is important to note that the investigated gold(III) complexes were stable in acetone, allowing an unobstructed recording of 2D NMR spectra.

The proton chemical shifts of the diazanaphthalene ligands in deuteroacetone generally agree with the literature values for the other solvents.[47–49] The ^{1}H NMR spectra of the gold(III) complexes **1–5** were noticeably different from those of the uncoordinated diazanaphthalene ligands; addition of the free ligand resulted in another set of ^{1}H signals with the expected chemical shifts. The auration of all ligands resulted in ^{1}H deshielding, with a mean value $\Delta_{H1–H8}$: +0.45–0.65 ppm, as deduced from the unassigned ^{1}H NMR data. The observed downfield shifts for complexes **1–5** with respect to the free diazanaphthalene ligands were a consequence of the strong electron-withdrawing effect of Au(III) ion; *i.e.* the overall electron density is shifted toward the AuCl$_3$ fragment, making diazanaphthalene ring electron-deficient compared to the uncoordinated ligand. Further evidence for the reduced nucleophilicity of the uncoordinated nitrogen atom in the investigated complexes is provided by DFT calculations (*vide infra*).

Coordination to Au(III) of phtz, 1,5-naph and 1,8-naph ligands resulted in the appearance of six sets of proton signals in the spectra of complexes **2**, **3** and **5**, respectively (three sets of proton signals are present in the spectra of free ligands). As an illustration of these findings, ^{1}H NMR spectra of free 1,8-naph ligand and the corresponding gold(III) complex **5** are presented in Fig. S1a.† Moreover, from the obtained NMR spectroscopic results, it can be concluded that qz and 1,6-naph ligands in the complexes **1** and **4** are exclusively coordinated through the N3 and N6 nitrogen atoms, respectively. This is clearly illustrated in Fig. S1b,† which shows the ^{1}H NMR spectra of the uncoordinated 1,6-naph and its complex **4**.

The Au(III) complexation of the diazanaphthalene ligands resulted in an overall deshielding of ring carbons, in some cases up to 7.8 ppm (mean $\Delta_{C1–C8a}$: +1.2–3.4 ppm). In the case of complex **2**, all carbon atoms were deshielded (up to 5.5 ppm). This is in accordance with downfield shifting of carbon signals previously found for [AuCl$_3$(pydz)] (pydz is pyridazine) complex; both these complexes contain two adjacent nitrogen atoms.[35]
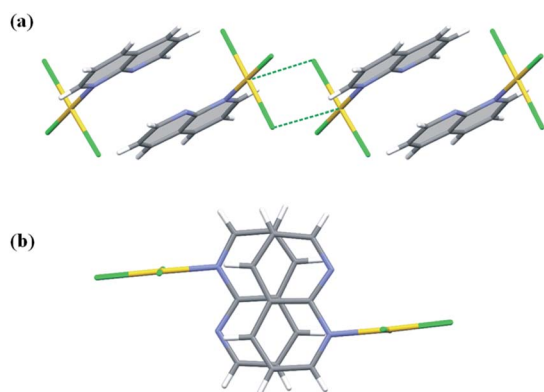

Fig. 7 Pairwise π···π and Au···Cl interactions between two symmetry independent molecules of complex **5** in non-centrosymmetric space group *Cc* (a); view perpendicular to the 1,8-naph plane displaying a degree of the ring overlap (b).

On the other hand, in the remaining four gold(III) complexes, nitrogen-adjacent carbons were shielded (up to −13.5 ppm for C8a, which is positioned between N1 and N8 atoms, in complex 5). These spectral characteristics were also previously noted for the mononuclear gold(III) complexes with monodentatedly coordinated pyrimidine,[35] pyrazine,[35] quinoxaline[36] and phenazine,[36] as well as for [Au(AMP)Cl₂]Cl·H₂O complex (AMP is bidentatedly coordinated 2-(aminomethyl)pyridine)[50] and some pyridinium cations.[51–53]

The UV-Vis spectra of the presently investigated gold(III) complexes 1–5 were recorded in acetone. The wavelengths of maximum absorption for 1–5 (λ_{max}, nm) and molar extinction coefficients (ε, M^{-1} cm^{-1}) determined right after dissolution of the complexes, are listed in the Experimental section. As can be expected, the shape of the spectra and values of λ_{max} are almost identical for all complexes indicating the same monodentate coordination mode of N-heterocycles. The UV-Vis data show absorption around 320.0 nm, which corresponds to LMCT (ligand-to-metal charge transfer) transitions and could be assigned to Cl → Au charge transfer by analogy to auric acid absorption spectra.[54–56]

Theoretical studies

In order to gain better understanding on the coordination mode of the investigated diazanaphthalenes toward the Au(III) ion, the structures of the ligands and corresponding gold(III) complexes 1–5 were optimized for the isolated molecules by means of DFT methods. Of the three experimental approaches (B3LYP, M06 and M06-2X, see Experimental section), the M06-2X method showed the best agreement with the corresponding crystallographic data. Consequently, this method was chosen for the structure optimization of the gold(III) complexes 1–5 and the investigated diazanaphthalenes. The calculated bond lengths (Å) and angles (°) for 1–5 are given in Table S2† and show a good agreement with the corresponding crystallographic data.

The donor ability of diazanaphthalenes toward Au(III) has been evaluated by observing the composition of the highest occupied molecular orbital (HOMO) and the molecular charge distribution, by using NBO analysis. The calculated NBO

charges (e) of donor nitrogen atoms and eigenvalues (hartree) of HOMOs and LUMOs of diazanaphthalenes are presented in Table 1. The results summarized in this table pointed out that electron-donating ability of diazanaphthalenes increases with increasing of the HOMOs eigenvalues[57–59] in the following order: 1,8-naph ≈ 1,5-naph < phtz < qz ≈ 1,6-naph. Furthermore, the nitrogen N3 and N6 atoms in asymmetrical qz and 1,6-naph ligands, respectively, are slightly more negatively charged than the corresponding N1 nitrogen.

To obtain more information about the favorable site of Au(III) electrophilic attack in these two ligands, we have examined their molecular electrostatic potential (MEP) mapped on the electron density surface generated at M06-2X/cc-pVTZ level of theory (Fig. 8a). The MEP has been shown so far as a very useful tool for prediction of the sites of electrophilic and nucleophilic attacks, as well as hydrogen bonding interactions.[38,60,61] The regions of the negative potentials, colored in red, are related to the possible sites of an electrophilic attack, while the regions of positive potential (blue) may indicate the sites of a nucleophilic attack.

As can be expected for the diazanaphthalene ligands, the negative potential regions are on the electronegative nitrogen atoms. The negative electrostatic potential values are −0.039 a.u. for N1 and −0.041 a.u. for N3 in qz, and −0.038 a.u. for N1 and −0.044 a.u. for N6 in 1,6-naph (Fig. 8a). Due to the fact that in both qz and 1,6-naph ligands the difference between the values of the electrostatic potential for the two nitrogens is not very large, we have optimized the structures and calculated the energies for the four distinct mononuclear gold(III) complexes, in which qz and 1,6-naph ligands are coordinated via either of the two nitrogen atoms. The structures of these complexes in the gas phase, calculated for the reaction of qz and 1,6-naph with an equimolar amount of [AuCl₄]⁻, are presented in Fig. 9 along with their relative energies. Gold(III) complexes with N1 coordinated nitrogen were calculated to be higher in energy by 1.1 and 2.6 kcal mol⁻¹, respectively, in comparison with the complexes 1 and 4 having N3 and N6 coordinated qz and 1,6-naph ligands, respectively. This undoubtedly confirms that the latter two complexes are energetically more favorable, being in agreement with our spectroscopic and crystallographic results.

Table 1 NBO charges (e) on the nitrogen atoms and eigenvalues (hartree) of HOMOs and LUMOs calculated for the diazanaphthalenes and the corresponding complexes 1–5 using DFT calculations at M06-2X/cc-pVTZ and M06-2X/(LanL2TZ(f)+cc-pVTZ) level of theory, respectively

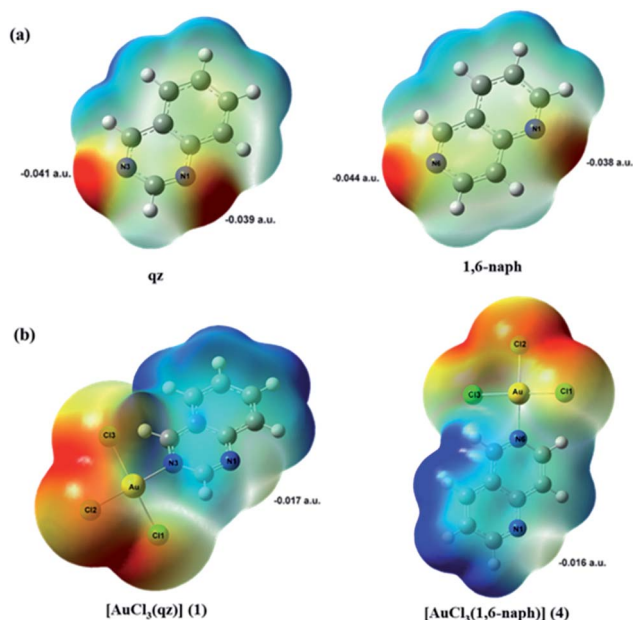| Ligand/gold(III) complex	q_{N1}	q_{N2}	q_{N3}	q_{N5}	q_{N6}	q_{N8}	E_{HOMO}	E_{LUMO}
qz	−0.446		−0.460				−0.3041	−0.0426
1	−0.414		−0.499				−0.3395	−0.1071
phtz[a]		−0.232	−0.232				−0.3091	−0.0403
2		−0.259	−0.191				−0.3271	−0.09283
1,5-naph[a]	−0.420			−0.420			−0.3150	−0.0421
3	−0.434			−0.404			−0.3377	−0.1036
1,6-naph	−0.423				−0.426		−0.3037	−0.0430
4	−0.417				−0.461		−0.3372	−0.1047
1,8-naph[a]	−0.404					−0.404	−0.3155	−0.0426
5	−0.430					−0.408	−0.3240	−0.0954

[a] Compound is symmetric.

Fig. 8 Electrostatic potential mapped on electron density surfaces for (a) asymmetrical qz and 1,6-naph ligands and (b) complexes **1** and **4** generated at DFT M06-2X/cc-pVTZ and M06-2X/(LanL2TZ(f)+cc-pVTZ) levels of theory, respectively (isoval 0.0004 a.u.). Color change from red most negative to blue most positive.

DFT calculations have been also used to provide an evidence that the presence of an electron-pulling AuCl₃ group bound to the nitrogen atom of diazanaphthalene ring makes it electron-deficient and reduces the nucleophilicity of the second nitrogen atom, preventing the formation of dinuclear gold(III) species. As can be seen from Table 1, coordination of all N-

Fig. 9 The calculated structures of the four mononuclear gold(III) complexes that could supposedly be formed as the final product of the reactions of (a) qz and (b) 1,6-naph with an equimolar amount of [AuCl₄]⁻, as well as their relative energies in the gas phase.

heterocycles to the Au(III) caused a decrease in the eigenvalues of the HOMOs, which indicates that the obtained mononuclear gold(III) complexes have lower electron-donating ability than the corresponding ligands. To obtain information about the potential sites in [AuCl₃(N-heterocycle)]] complexes, which can be a target of Au(III) electrophilic attack, their MEPs have been generated at M06-2X/(LanL2TZ(f)+cc-pVTZ) level of theory. The MEP maps for all investigated gold(III) complexes have shown that Au(III) ion bound to the heteroaromatic ring made it electron-deficient compared to the uncoordinated ligands. This has caused, as a consequence, an increase of the electrostatic potential value on the uncoordinated nitrogen atom; accordingly, this nitrogen is no longer a preferable site for the electrophilic attack of the subsequent AuCl₃ fragment. As an illustration of this finding, the MEPs for complexes **1** and **4** are presented in Fig. 8b.

Nonlinear optical (NLO) properties of complexes 1–5

In the last decades, many transition metal complexes have been gaining much attention as potential building blocks for second order nonlinear optical (NLO) materials.[62–64] Compared to organic molecules, metal complexes offer a larger variety of molecular structures in relation to metal nd configuration, oxidation and spin state, and can satisfy the different demands of second order NLO materials, such as switchable, tunable and multidimensional optical properties.[64]

It is well known that the nonlinear optical response of an isolated molecule in an electric field $E_i(\omega)$ can be presented as a Taylor series expansion of the total dipole moment, μ, induced by the field:

$$\mu = \mu_0 + \alpha_{ij}E_j + \beta_{ijk}E_jE_k + \ldots$$

where μ_0 is the permanent dipole moment, α is the linear polarizability and β_{ijk} are the first hyperpolarizability tensor components. The calculations of the total dipole moment (μ), the average polarizability (α) and the first hyperpolarizability (β) from the Gaussian 09 output have been explained in detail previously.[65,66]

The polar properties of the gold(III) complexes **1–5** were calculated at M06-2X/(LanL2TZ(f)+cc-pVTZ) level of theory in the gas phase and the obtained results are presented in Table 2. According to this table, the calculated α values for the investigated gold(III) complexes increase in the order: **5 < 3 < 4 < 2 < 1**, and the calculated β values follow the similar trend, *i.e.* **5 < 4 < 3 < 2 < 1**. Urea is one of the prototypical compounds used in the study of NLO properties of the molecules.[67] Therefore, urea was selected as a reference, and its μ, α and β values were calculated at M06-2X/cc-pVTZ level of theory. Almost all presently investigated gold(III) complexes have the greater α and β values than the corresponding values of urea (up to 6.5 and 4.3 times, respectively). The exception is the complex **5**, which has a slightly lower β value than that of urea (1.2 times). This indicates that gold(III) complexes with diazanaphthalenes **1–5** might be good candidates for NLO materials.

As revealed by the X-ray analysis (*vide supra*), the complexes that display the lowest values of the polarizability (α) and
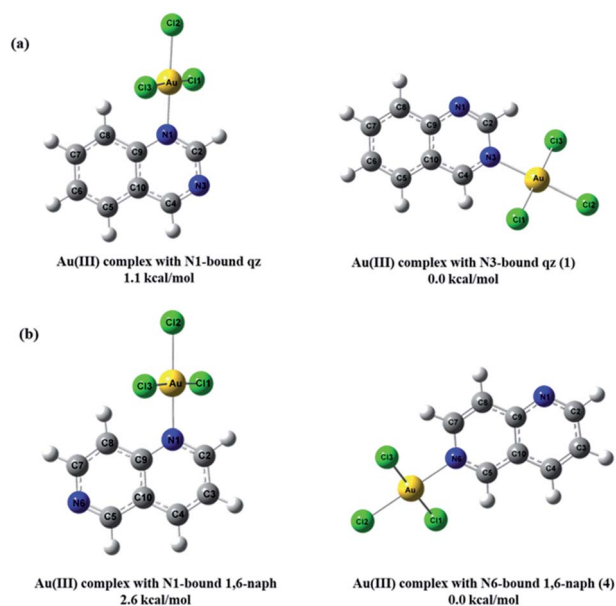
Table 2 The total dipole moment (μ), the average polarizability (α) and the first hyperpolarizability (β) calculated for the gold(III) complexes **1–5** using DFT calculations at M06-2X/(LanL2TZ(f)+cc-pVTZ) level of theory for the isolated molecules. Urea is presented as a reference

Compound	Dipole moment μ (D)	Polarizability α ($\times 10^{-24}$ esu)	Hyperpolarizability β ($\times 10^{-30}$ esu)
Urea[a]	4.3852	4.39	1.10
1	10.4442	28.36	4.73
2	13.7133	28.31	2.82
3	8.0700	27.51	2.29
4	10.1137	28.20	1.36
5	12.5106	27.46	0.94

[a] The presented values for urea are calculated at M06-2X/cc-pVTZ level of theory in the gas phase.

hyperpolarizability (β), namely **3**, **4** and **5**, form polar crystals. Polar crystals are of great interest because of their physical properties, such as pyroelectricity, ferroelectricity, piezoelectricity, second harmonic generation, which are only allowed in polar systems (crystalline or amorphous)[68] and are therefore highly requested in materials for advanced applications. Moreover, there is also a nice correlation between the value of the average polarizability (α) for the studied complex and its involvement in $\pi \cdots \pi$ stacking interactions in crystals. Namely, the highest α values are associated with the presence, while the lowest with the absence of $\pi \cdots \pi$ stacking. Indeed, the calculated correlation coefficient between the calculated polarizability (α) and the shortest distance between the planes defined by the diazanaphthalene fragments (h) (see Table S5†) is equal to -0.818. It means that the determination coefficient equal to 0.669 and the calculated polarizability (α) explain 66.9% of observed variation in the values of distances between planes defined by diazanaphthalene fragments (h). Unfortunately, due to the lack of the material, we were not able to perform the second-harmonic generation (SHG) measurements.

Experimental

Materials and measurements

Potassium tetrachloridoaurate(III) (K[AuCl₄]), quinazoline (qz), dichloromethane, ethanol, acetone and deuteroacetone were purchased from the Sigma-Aldrich Chemical Co. Phthalazine (phtz), 1,5-naphthyridine (1,5-naph), 1,6-naphthyridine (1,6-naph) and 1,8-naphthyridine (1,8-naph) were obtained from abcr GmbH & Co. KG. All the employed chemicals were of analytical reagent grade and used without further purification.

Elemental microanalyses for carbon, hydrogen and nitrogen were performed on a Vario EL instrument by the Microanalytical Laboratory, Department of Organic Chemistry, University of Heidelberg. All NMR spectra were recorded at 25 °C in acetone-d₆ on a Bruker Avance II 400 MHz spectrometer. Chemical shifts are reported in ppm (δ) and scalar couplings are reported in Hertz. 5.0 mg of each compound was dissolved in 0.6 mL of acetone-d₆ and transferred into a 5 mm NMR tube. The splittings are designated as: s, singlet; d, doublet; m, multiplet; dd,

doublet of doublets; dt, doublet of triplets; td, triplet of doublets; ddd, doublet of doublet of doublets. The UV-Vis spectra were recorded on a Jasco V570 spectrophotometer after dissolving the corresponding gold(III) complex in acetone, over the wavelength range 600–200 nm. The concentration of the gold(III) complexes was 2.5×10^{-4} M.

Synthesis of the gold(III) complexes 1–5

Gold(III) complexes with five isomeric dizanaphthalenes were synthesized according to the modified procedure published in the literature for the preparation of [AuCl₃(N-heterocycle)] complexes (N-heterocycle is pyridazine, pyrimidine, pyrazine, quinoxaline, phenazine, 1,7- and 4,7-phenanthroline, and methylcamphorquinoxaline derivatives).[35–38]

The solution of 0.5 mmol of the corresponding diazanaphthalene ligand (65.1 mg) in 2.0 mL of ethanol was added slowly under stirring to the solution containing an equimolar amount of K[AuCl₄] (188.9 mg) in 10.0 mL of water. The yellow precipitate, formed immediately after addition of the N-heterocyclic ligand, was filtered off, washed with water, and recrystallized in dichloromethane to form yellow crystals of gold(III) complexes **1–5**. The crystals were collected from the solution and dried in the dark at ambient temperature. The yield was 69% for [AuCl₃(qz)] (**1**) (149.5 mg), 65% for [AuCl₃(phtz)] (**2**) (140.9 mg), 54% for [AuCl₃(1,5-naph)] (**3**) (117.0 mg), 43% for [AuCl₃(1,6-naph)] (**4**) (93.2 mg) and 58% for [AuCl₃(1,8-naph)] (**5**) (125.7 mg).

Anal. calcd for **1** = C₈H₆AuCl₃N₂ (MW = 433.46): C, 22.17; H, 1.40; N, 6.46. Found: C, 22.13; H, 1.46; N, 6.51%. ¹H NMR (400 MHz, CD₃COCD₃): 8.13 (ddd, J = 8.1, 7.1, 1.0 Hz, H6), 8.29 (dd, J = 8.5, 0.6 Hz, H7), 8.47 (ddd, J = 8.5, 7.0, 1.4 Hz, H5), 8.59 (dd, J = 8.3, 0.7 Hz, H8), 9.64 (s, H4), 10.32 (s, H2) ppm. ¹³C NMR (101 MHz, CD₃COCD₃): 125.4 (C8a), 128.2 (C7), 130.4 (C8), 131.2 (C6), 140.0 (C5), 149.8 (C4a), 150.6 (C4), 162.2 (C2) ppm. UV-Vis (acetone, λ_{max}, nm): 323.0 (ε = 4.0 × 10³ M⁻¹ cm⁻¹).

Quinazoline (qz)*: ¹H NMR (400 MHz, CD₃COCD₃): 7.76 (ddd, J = 8.1, 4.5, 3.5 Hz, H6), 8.02 (dd, J = 4.7, 1.1 Hz, H5 and H7), 8.13 (dt, J = 8.2, 1.0 Hz, H8), 9.26 (s, H4), 9.54 (s, H2) ppm. ¹³C NMR (101 MHz, CD₃COCD₃): 125.2 (C8a), 127.6 (C6), 127.9 (C8), 128.1 (C7), 134.1 (C5), 149.9 (C4a), 155.2 (C4), 160.4 (C2) ppm.

Anal. calcd for **2** = C₈H₆AuCl₃N₂ (MW = 433.46): C, 22.17; H, 1.40; N, 6.46. Found: C, 22.10; H, 1.53; N, 6.56%. ¹H NMR (400 MHz, CD₃COCD₃): 8.45 (ddd, J = 8.2, 7.1, 1.3 Hz, H6), 8.53 (ddd, J = 8.2, 7.1, 1.2 Hz, H7), 8.61 (dd, J = 8.2, 1.0 Hz, H5), 8.69 (dd, J = 8.0, 0.8 Hz, H8), 9.90 (s, H4), 10.47 (s, H1) ppm. ¹³C NMR (101 MHz, CD₃COCD₃): 127.6 (C8a), 127.9 (C5), 129.2 (C8), 129.7 (C4a), 135.2 (C6), 138.1 (C7), 155.0 (C4), 156.2 (C1) ppm. UV-Vis (acetone, λ_{max}, nm): 323.0 (ε = 3.7 10³ M⁻¹ cm⁻¹).

Phthalazine (phtz): ¹H NMR (400 MHz, CD₃COCD₃): 8.05 (dd, J = 6.0, 3.2 Hz, H6 and H7), 8.18 (dd, J = 6.0, 3.6 Hz, H5 and H8), 9.65 (s, H1 and H4) ppm. ¹³C NMR (101 MHz, CD₃COCD₃): 126.3 (C5 and C8), 126.4 (C4a and C8a), 132.6 (C6 and C7), 150.8 (C1 and C4) ppm.

Anal. calcd for **3** = C₈H₆AuCl₃N₂ (MW = 433.46): C, 22.17; H, 1.40; N, 6.46. Found: C, 22.02; H, 1.58; N, 6.58%. ¹H NMR (400

MHz, CD$_3$COCD$_3$): 8.28 (dd, J = 8.8, 4.0 Hz, H7), 8.44 (dd, J = 8.5, 5.5 Hz, H3), 9.13 (d, J = 8.4 Hz, H4), 9.31 (d, J = 8.8 Hz, H8), 9.36 (dd, J = 4.0, 1.2 Hz, H6), 9.86 (dd, J = 5.6, 1.2 Hz, H2) ppm. ^{13}C NMR (101 MHz, CD$_3$COCD$_3$): 127.6 (C3), 128.1 (C7), 134.1 (C8), 143.1 (C8a), 144.9 (C4), 145.4 (C4a), 154.1 (C2), 154.2 (C6) ppm. UV-Vis (acetone, λ_{max}, nm): 323.0 (ε = 4.3 × 10^3 M^{-1} cm^{-1}).

1,5-Naphthyridine (1,5-naph): ^{1}H NMR (400 MHz, CD$_3$-COCD$_3$): 7.79 (dd, J = 8.4, 4.0 Hz, H3 and H7), 8.43 (m), 9.02 (dd, J = 4.0, 1.5 Hz, H2 and H6) ppm. ^{13}C NMR (101 MHz, CD$_3$-COCD$_3$): 124.5 (C3 and C7), 137.1 (C4 and C8), 143.9 (C4a and C8a), 151.3 (C2 and C6) ppm.

Anal. calcd for **4** = C$_8$H$_6$AuCl$_3$N$_2$ (MW = 433.46): C, 22.17; H, 1.40; N, 6.46. Found: C, 22.29; H, 1.54; N, 6.34%. ^{1}H NMR (400 MHz, CD$_3$COCD$_3$): 8.05 (dd, J = 8.5, 4.3 Hz, H3), 8.46 (d, J = 6.9 Hz, H8), 8.98 (d, J = 8.5 Hz, H4), 9.18 (d, J = 6.1 Hz, H7), 9.50 (dd, J = 4.3, 1.7 Hz, H2), 10.13 (s, H5) ppm. ^{13}C NMR (101 MHz, CD$_3$COCD$_3$): 124.8 (C4a), 125.6 (C3), 127.0 (C8), 138.4 (C4), 144.9 (C7), 156.4 (C5 and C8a), 160.0 (C2) ppm. UV-Vis (acetone, λ_{max}, nm): 322.0 (ε = 2.3 × 10^3 M^{-1} cm^{-1}).

1,6-Naphthyridine (1,6-naph): ^{1}H NMR (400 MHz, CD$_3$-COCD$_3$): 7.71 (dd, J = 8.4, 4.4 Hz, H3), 7.92 (d, J = 6.0 Hz, H8), 8.56 (ddd, J = 8.3, 1.7, 0.8 Hz, H4), 8.77 (d, J = 6.0 Hz, H7), 9.15 (dd, J = 4.2, 1.7 Hz, H2), 9.39 (s, H5) ppm. ^{13}C NMR (101 MHz, CD$_3$COCD$_3$): 122.7 (C8), 123.8 (C3), 124.7 (C4a), 136.6 (C4), 147.6 (C7), 151.3 (C8a), 154.1 (C5), 155.9 (C2) ppm.

Anal. calcd for **5** = C$_8$H$_6$AuCl$_3$N$_2$ (MW = 433.46): C, 22.17; H, 1.40; N, 6.46. Found: C, 22.20; H, 1.58; N, 6.49%. ^{1}H NMR (400 MHz, CD$_3$COCD$_3$): 8.09 (dd, J = 8.2, 4.2 Hz, H5), 8.29 (dd, J = 8.0, 5.6 Hz, H4), 8.90 (dd, J = 8.0, 1.2 Hz, H6), 9.20 (d, J = 8.0 Hz, H3), 9.43 (d, J = 2.8 Hz, H7), 9.81 (d, J = 5.2 Hz, H2) ppm. ^{13}C NMR (101 MHz, CD$_3$COCD$_3$): 125.6 (C5), 126.2 (C4), 127.2 (C4a), 140.0 (C6), 143.8 (C8a), 146.0 (C3), 156.1 (C2), 157.4 (C7) ppm. UV-Vis (acetone, λ_{max}, nm): 323.0 (ε = 3.4 × 10^3 M^{-1} cm^{-1}).

1,8-Naphthyridine (1,8-naph): ^{1}H NMR (400 MHz, CD$_3$-COCD$_3$): 7.64 (dd, J = 8.2, 4.2 Hz, H4 and H5), 8.46 (dd, J = 8.0, 2.0 Hz, H3 and H6), 9.13 (dd, J = 4.0, 2.0 Hz, H2 and H7) ppm. ^{13}C NMR (101 MHz, CD$_3$COCD$_3$): 123.1 (C4 and C5), 123.9 (C4a), 138.2 (C3 and C6), 154.3 (C2 and C7), 157.3 (C8a) ppm.

* NMR data for the free ligands are given for comparative purposes.

Crystallographic data collection and refinement of the structures

X-ray measurements were carried out at 295 K with Mo Kα radiation (λ = 0.71073 Å) on Xcalibur kappa-geometry diffractometer equipped with Eos CCD detector using CrysAlisPro software.[69] Analytical numeric absorption correction using a multifaceted crystal model based on expressions derived by Clark & Reid[70] was applied. Further crystallographic and refinement data can be found in Table S1.† The structures were solved by direct methods using SHELXT[71] and refined by full-matrix least-squares calculations on F^2 with SHELXL.[72] Anisotropic displacement parameters were refined for all non-hydrogen atoms. The positions of the hydrogen atoms attached to the carbon atoms were calculated at standardized

distances (0.93 Å) and refined using a riding model with isotropic displacement parameters 20% higher than the isotropic equivalent of their carriers. Crystals of **3** and **5** were refined as racemic twins with a ratio of twin components 0.608 : 0.392 and 0.442 : 558, respectively. MERCURY[45] computer graphics program was used to prepare drawings.

Quantum-mechanical calculations

The M06, M06-2X and B3LYP density functional theory methods were used in our calculations. The M06 and M06-2X methods are the hybrid meta-GGA functionals, where the Hartree–Fock exchange energy (X) is equal to 27 and 54% respectively.[73] The B3LYP consists of Becke three-parameter hybrid exchange functional (B3)[74] and the Lee, Yang, and Parr correlation functional (LYP) at the gradient-corrected DFT level.[75] The B3LYP and M06 functionals are known to give good descriptions of transition metal complexes,[73,76–78] while the M06-2X are recommended for the aromatic nitrogen-containing heterocycles.[79] The basis set for calculations on diazanaphthalenes was Dunning's correlation consistent polarized valence double-ζ (cc-pVDZ) basis set,[80] while for calculations for gold(III) complexes the basis set was composite: cc-pVDZ basis set for the hydrogen, nitrogen, carbon and chlorine[80] and LanL2TZ(f) basis set for gold atom.[81] The latter contains the LanL2 relativistic effective core potential (RECP) of Hay and Wadt[71] and a flexible triple-ζ basis set augmented with f polarization functions in the treatment of valence shell on the Au atom. All structures were fully optimized without any geometric constraints. To check the influence of basis set effects for each optimized geometry of the diazanaphthalenes and gold(III) complexes, the additional single-point calculations were completed at the M06-2X/cc-pVTZ and M06-2X/(LanL2TZ(f)+cc-pVTZ) levels of theory, respectively (cc-pVTZ is correlation consistent polarized valence triple-ζ basis set[80]). The optimized structures were confirmed to be potential energy minima by vibrational frequency calculations at the same level of theory because no imaginary frequency was found. The natural bond analyses (NBO)[82] were performed at M06-2X/cc-pVTZ and M06-2X/(LanL2TZ(f)+cc-pVTZ) levels of theory in order to provide indices of the diazanaphthalenes and gold(III) complexes, respectively. Finally, polarizability and hyperpolarizability calculations for the gold(III) complexes were performed at M06-2X/(LanL2TZ(f)+cc-pVTZ) level of theory. All DFT calculations were performed using the Gaussian 09 program package.[83] The M06, M06-2X and B3LYP methods, as well as cc-pVDZ and cc-pVTZ basis sets were employed as implemented in the software package, while the LanL2TZ(f) basis set for gold was obtained from EMSL Basis set Exchange.[84]

Conclusions

Although ligands with hypodentate coordination mode are known to increase their denticity when a coligand can be expelled from the metal coordination sphere, this is not taking place in [AuCl$_3$(L)] complexes with aromatic diazaheterocycles (L). In the investigated series of Au(III) complexes, the dipodal

diazanaphthalene ligands always act as monodentate. This seems to be a consequence of an increase of the electrostatic potential value on the uncoordinated nitrogen atom upon coordination of diazanaphthalene. Whenever in the diazaaromatic ligand the two sites available for coordination are nonequivalent (as in qz and 1,6-naph ligands), the Au–N bond is formed to the nitrogen atom in the naphthalene β position. This coordination mode eases the columnar $\pi\cdots\pi$ stacking interactions between the heteroaromatic rings in crystals. Crystallographic studies indicate the presence of the extended 4 + 1 or 4 + 2 geometry around the Au(III) center, mainly due to Au$\cdots$Cl, but also due to Au$\cdots$N interactions, and the importance of Cl$\cdots$Cl contacts and C–H$\cdots$Cl, and C–H$\cdots$N hydrogen bonds as specific tools for organizing all these molecules in the solid state. On the other hand, the structure-determining role of $\pi\cdots\pi$ stacking between diazaaromatic ligands is unambiguous only in [AuCl$_3$(benzodiazine)] complexes, which form centrosymmetric crystals and appears vague in the crystals formed by [AuCl$_3$(naphthyridine)] complexes, which arrange into noncentrosymmetric polar aggregates. Interestingly, the molecules belonging to the latter group display the lowest values of polarizability (α) and hyperpolarizability (β). These results suggest that, in the investigated series of complexes, the dispersion contributions to the aromatic $\pi\cdots\pi$ interaction are significant.

Conflicts of interest

There are no conflicts to declare.

Acknowledgements

Notes and references

1 M. S. Butler, *J. Nat. Prod.*, 2004, **67**, 2141.

2 J. A. Joule and K. Mills, *Heterocyclic Chemistry*, Blackwell Science, Oxford, 2000.

3 V. K. Indirapriyadharshini, P. Ramamurthy, V. Raghukumar and V. T. Ramakrishnan, *Spectrochim. Acta, Part A*, 2002, **58**, 1535.

4 S. Derossi, M. Casanova, E. Iengo, E. Zangrando, M. Stener and E. Alessio, *Inorg. Chem.*, 2007, **46**, 11243.

5 M. Schweiger, S. R. Seidel, A. M. Arif and P. J. Stang, *Angew. Chem., Int. Ed.*, 2001, **113**, 3575.

6 M. Willermann, C. Mulcahy, R. K. O. Sigel, M. M. Cerdà, E. Freisinger, P. J. Sanz Miguel, M. Roitzsch and B. Lippert, *Inorg. Chem.*, 2006, **45**, 2093.

7 C. J. Sumby, *Coord. Chem. Rev.*, 2011, **255**, 1937.

8 C. Kaes, A. Katz and M. W. Hosseini, *Chem. Rev.*, 2000, **100**, 3553.

9 P. J. Steel, *Coord. Chem. Rev.*, 1990, **106**, 227.

10 D. P. Ašanin, M. D. Živković, S. Rajković, B. Warżajtis, U. Rychlewska and M. I. Djuran, *Polyhedron*, 2013, **51**, 255.

11 S. Rajković, D. P. Ašanin, M. D. Živković and M. I. Djuran, *Polyhedron*, 2013, **65**, 42.

12 S. Rajković, U. Rychlewska, B. Warżajtis, D. P. Ašanin, M. D. Živković and M. I. Djuran, *Polyhedron*, 2014, **67**, 279.

13 V. Balzani, A. Juris, M. Venturi, S. Campagna and S. Serroni, *Chem. Rev.*, 1996, **96**, 759.

14 D. E. Fenton, *Chem. Soc. Rev.*, 1999, **28**, 159.

15 A. M. Barrios and S. J. Lippard, *Inorg. Chem.*, 2001, **40**, 1250.

16 A. M. Barrios and S. J. Lippard, *Inorg. Chem.*, 2001, **40**, 1060.

17 B. Bertrand and A. Casini, *Dalton Trans.*, 2014, **43**, 4209.

18 B. Đ. Glišić and M. I. Djuran, *Dalton Trans.*, 2014, **43**, 5950.

19 K. Palanichamy, N. Sreejayan and A. C. Ontko, *J. Inorg. Biochem.*, 2012, **106**, 32.

20 L. Messori, F. Abbate, G. Marcon, P. Orioli, M. Fontani, E. Mini, T. Mazzei, S. Carotti, T. O'Connell and P. Zanello, *J. Med. Chem.*, 2000, **43**, 3541.

21 G. Marcon, S. Carotti, M. Coronnello, L. Messori, E. Mini, P. Orioli, T. Mazzei, M. A. Cinellu and G. Minghetti, *J. Med. Chem.*, 2002, **45**, 1672.

22 L. Messori, G. Marcon, M. A. Cinellu, M. Coronnelo, E. Mini, C. Gabbiani and P. Orioli, *Bioorg. Med. Chem.*, 2004, **12**, 6039.

23 A. Casini, M. A. Cinellu, G. Minghetti, C. Gabbiani, M. Coronnello, E. Mini and L. Messori, *J. Med. Chem.*, 2006, **49**, 5524.

24 C. Gabbiani, A. Casini, L. Messori, A. Guerri, M. A. Cinellu, G. Minghetti, M. Corsini, C. Rosani, P. Zanello and M. Arca, *Inorg. Chem.*, 2008, **47**, 2368.

25 A. N. Wein, A. T. Stockhausen, K. I. Hardcastle, M. R. Saadein, S. Peng, D. Wang, D. M. Shin, Z. Chen and J. F. Eichler, *J. Inorg. Biochem.*, 2011, **105**, 663.

26 R. W.-Y. Sun and C.-M. Che, *Coord. Chem. Rev.*, 2009, **253**, 1682.

27 C. T. Lum, A. S.-T. Wong, M. Lin, C.-M. Che and R. W.-Y. Sun, *Chem. Commun.*, 2013, **49**, 4364.

28 R. D. Teo, H. B. Gray, P. Lim, J. Termini, E. Domeshek and Z. Gross, *Chem. Commun.*, 2014, **50**, 13789.

29 N. D. Savić, D. R. Milivojevic, B. Đ. Glišić, T. Ilic-Tomic, J. Veselinovic, A. Pavic, B. Vasiljevic, J. Nikodinovic-Runic and M. I. Djuran, *RSC Adv.*, 2016, **6**, 13193.

30 C. Gabbiani, L. Messori, M. A. Cinellu, A. Casini, P. Mura, A. R. Sannella, C. Severini, G. Majori, A. R. Bilia and F. F. Vincieri, *J. Inorg. Biochem.*, 2009, **103**, 310.

31 M. Navarro, C. Hernández, I. Colmenares, P. Hernández, M. Fernández, A. Sierraalta and E. Marchán, *J. Inorg. Biochem.*, 2007, **101**, 111.

32 S. P. Fricker, R. M. Mosi, B. R. Cameron, I. Baird, Y. Zhu, V. Anastassov, J. Cox, P. S. Doyle, E. Hansell, G. Lau, J. Langille, M. Olsen, L. Qin, R. Skerlj, R. S. Y. Wong,

Z. Santucci and J. H. McKerrow, *J. Inorg. Biochem.*, 2008, **102**, 1839.

33 R. A. Sánchez-Delgado, M. Navarro, K. Lazardi, R. Atencio, M. Capparelli, F. Vargas, J. A. Urbina, A. Bouillez, A. F. Noels and D. Masi, *Inorg. Chim. Acta*, 1998, **275–276**, 528.

34 E. Nyarko, T. Hara, D. J. Grab, A. Habib, Y. Kim, O. Nikolskaia, T. Fukuma and M. Tabata, *Chem.-Biol. Interact.*, 2004, **148**, 19.

35 B. Warżajtis, B. Đ. Glišić, N. S. Radulović, U. Rychlewska and M. I. Djuran, *Polyhedron*, 2014, **79**, 221.

36 B. Đ. Glišić, B. Warżajtis, N. S. Radulović, U. Rychlewska and M. I. Djuran, *Polyhedron*, 2015, **87**, 208.

37 A. Pavic, B. Đ. Glišić, S. Vojnovic, B. Warżajtis, N. D. Savić, M. Antić, S. Radenković, G. V. Janjić, J. Nikodinovic-Runic, U. Rychlewska and M. I. Djuran, *J. Inorg. Biochem.*, 2017, **174**, 156.

38 B. Đ. Glišić, M. Hoffmann, B. Warżajtis, M. S. Genčić, P. D. Blagojević, N. S. Radulović, U. Rychlewska and M. I. Djuran, *Polyhedron*, 2016, **105**, 137.

39 C. R. Groom, I. J. Bruno, M. P. Lightfoot and S. C. Ward, *Acta Crystallogr., Sect. B: Struct. Sci., Cryst. Eng. Mater.*, 2016, **72**, 171.

40 J. Bernstein, R. E. Davis, L. Shimoni and N.-L. Chang, *Angew. Chem., Int. Ed.*, 1995, **34**, 1555.

41 G. R. Desiraju, P. Shing Ho, L. Kloo, A. C. Legon, R. Marquardt, P. Metrangolo, P. Politzer, G. Resnati and K. Rissanen, *Pure Appl. Chem.*, 2013, **85**, 1711.

42 Ch. Janiak, *J. Chem. Soc., Dalton Trans.*, 2000, 3885.

43 G. R. Desiraju and R. J. Parthasarathy, *J. Am. Chem. Soc.*, 1989, **111**, 8725.

44 T. P. Andrejević, B. Warżajtis, B. Đ. Glišić, S. Vojnovic, M. Mojicevic, N. Lj. Stevanović, J. Nikodinovic-Runic, U. Rychlewska and M. I. Djuran, *J. Inorg. Biochem.*, 2020, **208**, 111089.

45 C. F. Macrae, P. R. Edgington, P. McCabe, E. Pidcock, G. P. Shields, R. Taylor, M. Towler and J. van de Streek, *J. Appl. Crystallogr.*, 2006, **39**, 453.

46 A. I. Kitaigorodskii, *Organic Chemical Crystallography*, Consultant's Bureau, New York, 1961.

47 S. Zhu, K. X. Moreno, R. M. Jenkins and J. A. Walmsley, *Dalton Trans.*, 2008, 6401.

48 P. J. Black and M. L. Heffernan, *Aust. J. Chem.*, 1965, **18**, 707.

49 W. W. Paudler and T. J. Kress, *J. Heterocyclic Chem.*, 1965, **2**, 393.

50 B. Warżajtis, B. Đ. Glišić, M. D. Živković, S. Rajković, M. I. Djuran and U. Rychlewska, *Polyhedron*, 2015, **91**, 35.

51 D. Niedzielska, T. Pawlak, M. Bozejewicz, A. Wojtczak, L. Pazderski and E. Szłyk, *J. Mol. Struct.*, 2013, **1032**, 195.

52 A. Pevec and A. Demšar, *J. Fluorine Chem.*, 2008, **129**, 707.

53 A. Pevec, M. Tekavec and A. Demšar, *Polyhedron*, 2011, **30**, 549.

54 K. Esumi, M. Nawa, N. Aihara and K. Usui, *New J. Chem.*, 1998, **22**, 719.

55 N. Pantelić, B. B. Zmejkovski, J. Trifunović-Macedoljan, A. Savić, D. Stanković, A. Damjanović, Z. Juranić,

G. N. Kaluđerović and T. J. Sabo, *J. Inorg. Biochem.*, 2013, **128**, 146.

56 N. Pantelić, T. P. Stanojković, B. B. Zmejkovski, T. J. Sabo and G. N. Kaluđerović, *Eur. J. Med. Chem.*, 2015, **90**, 766.

57 P. Tyagi, S. Chandra, B. S. Saraswat and D. Sharma, *Spectrochim. Acta, Part A*, 2015, **143**, 1.

58 H. Hu, L. Du, X. Li, H. Zhao, X. Zhang, S. Shi, H. Li, X. Tang and J. Yang, *Int. J. Electrochem. Sci.*, 2013, **8**, 11228.

59 Y.-H. Zhou, J. Tao, D.-L. Sun, L.-Q. Chen, W.-G. Ji and Y. Cheng, *Polyhedron*, 2015, **85**, 849.

60 F. J. Luque, J. M. López and M. Orozco, *Theor. Chem. Acc.*, 2000, **103**, 343.

61 R. V. Pinjari and S. P. Gejji, *J. Phys. Chem. A*, 2008, **112**, 12679.

62 Y.-X. Sun, Q.-L. Hao, W.-X. Wei, Z.-X. Yu, L.-D. Lu, X. Wang and Y.-S. Wang, *J. Mol. Struct.: THEOCHEM*, 2009, **904**, 74.

63 L. Pilia, M. Pizzotti, F. Tessore and N. Robertson, *Inorg. Chem.*, 2014, **53**, 4517.

64 S. Di Bella, *Chem. Soc. Rev.*, 2001, **30**, 355.

65 K. S. Thanthiriwatte and K. M. N. de Silva, *J. Mol. Struct.: THEOCHEM*, 2002, **617**, 169.

66 A. Esme and S. G. Sagdinc, *J. Mol. Struct.*, 2013, **1048**, 185.

67 K. Sayin and D. Karakaş, *Spectrochim. Acta, Part A*, 2015, **144**, 176.

68 T. Hahn and H. Klapper, Point groups and crystal classes, in *International Tables for Crystallography*, ed. T. Hahn and D. Reidel, Publishing Company, Dordrecht, Holland, 1983, vol. A, p. 746.

69 *CrysAlis PRO*, Agilent Technologies, Yarnton, Oxfordshire, England, 2014.

70 R. C. Clark and J. S. Reid, *Acta Crystallogr., Sect. A: Found. Crystallogr.*, 1995, **51**, 887.

71 G. M. Sheldrick, *Acta Crystallogr., Sect. A: Found. Adv.*, 2015, **71**, 3.

72 G. M. Sheldrick, *Acta Crystallogr., Sect. C: Struct. Chem.*, 2015, **71**, 3.

73 Y. Zhao and D. G. Truhlar, *J. Chem. Phys.*, 2006, **125**, 194101.

74 A. D. Becke, *J. Chem. Phys.*, 1993, **98**, 5648.

75 C. Lee, W. Yang and R. G. Parr, *Phys. Rev. B*, 1988, **37**, 785.

76 S. Q. Niu and M. B. Hall, *Chem. Rev.*, 2000, **100**, 353.

77 A. P. Martins, A. Marrone, A. Ciancetta, A. G. Cobo, M. Echevarría, T. F. Moura, N. Re, A. Casini and G. Soveral, *PLoS One*, 2012, **7**, e37435.

78 Y. Zhao and D. G. Truhlar, *Chem. Phys. Lett.*, 2011, **502**, 1.

79 R. G. A. R. Maclagan, S. Gronert and M. Meot-Ner, *J. Phys. Chem. A*, 2015, **119**, 127.

80 (*a*) T. H. Dunning Jr, *J. Chem. Phys.*, 1989, **90**, 1007; (*b*) D. E. Woon and T. H. Dunning Jr, *J. Chem. Phys.*, 1993, **98**, 1358.

81 P. J. Hay and W. R. Wadt, *J. Chem. Phys.*, 1985, **82**, 270.

82 (*a*) A. E. Reed and F. Weinhold, *J. Chem. Phys.*, 1983, **78**, 4066; (*b*) A. E. Reed, R. B. Weinstock and F. Weinhold, *J. Chem. Phys.*, 1985, **83**, 735; (*c*) A. E. Reed, L. A. Curtiss and F. Weinhold, *Chem. Rev.*, 1988, **88**, 899.

83 M. J. Frisch, G. W. Trucks, H. B. Schlegel, G. E. Scuseria, M. A. Robb, J. R. Cheeseman, G. Scalmani, V. Barone, B. Mennucci, G. A. Petersson, H. Nakatsuji, M. Caricato, X. Li, H. P. Hratchian, A. F. Izmaylov, J. Bloino, G. Zheng,

J. L. Sonnenberg, M. Hada, M. Ehara, K. Toyota, R. Fukuda, J. Hasegawa, M. Ishida, T. Nakajima, Y. Honda, O. Kitao, H. Nakai, T. Vreven, J. A. Montgomery Jr, J. E. Peralta, F. Ogliaro, M. Bearpark, J. J. Heyd, E. Brothers, K. N. Kudin, V. N. Staroverov, T. Keith, R. Kobayashi, J. Normand, K. Raghavachari, A. Rendell, J. C. Burant, S. S. Iyengar, J. Tomasi, M. Cossi, N. Rega, J. M. Millam, M. Klene, J. E. Knox, J. B. Cross, V. Bakken, C. Adamo, J. Jaramillo, R. Gomperts, R. E. Stratmann, O. Yazyev, A. J. Austin, R. Cammi, C. Pomelli, J. W. Ochterski, R. L. Martin, K. Morokuma, V. G. Zakrzewski, G. A. Voth, P. Salvador, J. J. Dannenberg, S. Dapprich, A. D. Daniels, O. Farkas, J. B. Foresman, J. V. Ortiz, J. Cioslowski and D. J. Fox, *Gaussian 09, Revision D.01*, Gaussian, Inc., Wallingford CT, 2013.

84 (*a*) D. Feller, *J. Comp. Chem.*, 1996, **17**, 1571; (*b*) K. L. Schuchardt, B. T. Didier, T. Elsethagen, L. Sun, V. Gurumoorthi, J. Chase, J. Li and T. L. Windus, *J. Chem. Inf. Model.*, 2007, **47**, 1045.